Methane observations from the Greenhouse Gases Observing SATellite: Comparison to ground-based TCCON data and model calculations

Robert Parker,[1] Hartmut Boesch,[1] Austin Cogan,[1] Annemarie Fraser,[2] Liang Feng,[2] Paul I. Palmer,[2] Janina Messerschmidt,[3] Nicholas Deutscher,[3,4] David W. T. Griffith,[4] Justus Notholt,[3] Paul O. Wennberg,[5] and Debra Wunch[5]

Received 20 April 2011; revised 21 June 2011; accepted 27 June 2011; published 6 August 2011.

[1] We report new short-wave infrared (SWIR) column retrievals of atmospheric methane (X_{CH4}) from the Japanese Greenhouse Gases Observing SATellite (GOSAT) and compare observed spatial and temporal variations with correlative ground-based measurements from the Total Carbon Column Observing Network (TCCON) and with the global 3-D GEOS-Chem chemistry transport model. GOSAT X_{CH4} retrievals are compared with daily TCCON observations at six sites between April 2009 and July 2010 (Bialystok, Park Falls, Lamont, Orleans, Darwin and Wollongong). GOSAT reproduces the site-dependent seasonal cycles as observed by TCCON with correlations typically between 0.5 and 0.7 with an estimated single-sounding precision between 0.4–0.8%. We find a latitudinal-dependent difference between the X_{CH4} retrievals from GOSAT and TCCON which ranges from 17.9 ppb at the most northerly site (Bialystok) to −14.6 ppb at the site with the lowest latitude (Darwin). We estimate that the mean smoothing error difference included in the GOSAT to TCCON comparisons can account for 15.7 to 17.4 ppb for the northerly sites and for 1.1 ppb at the lowest latitude site. The GOSAT X_{CH4} retrievals agree well with the GEOS-Chem model on annual (August 2009 – July 2010) and monthly timescales, capturing over 80% of the zonal variability. Differences between model and observed X_{CH4} are found over key source regions such as Southeast Asia and central Africa which will be further investigated using a formal inverse model analysis.
Citation: Parker, R., et al. (2011), Methane observations from the Greenhouse Gases Observing SATellite: Comparison to ground-based TCCON data and model calculations, *Geophys. Res. Lett.*, *38*, L15807, doi:10.1029/2011GL047871.

1. Introduction

[2] Methane is the second most important anthropogenic greenhouse gas, with a radiative forcing that is comparable to CO_2 over a 20-year horizon. Methane also influences tropospheric ozone and water vapor, further increasing its importance to the Earth's radiative budget. Recent unexpected changes in surface concentrations of CH_4 emphasize gaps in our current understanding of the CH_4 budget [*Bousquet et al.*, 2006; *Rigby et al.*, 2008; *Dlugokencky et al.*, 2009], which has relied on highly accurate but sparse ground-based measurements. Satellite observations of CH_4 offer new insights into the magnitude of regional sources and sinks and can help overcome large uncertainties associated with the upscaling and interpretation of surface concentration data.

[3] The usefulness of short-wave infrared (SWIR) measurements for inverse modeling has been demonstrated with the SCIAMACHY instrument onboard ENVISAT [*Bergamaschi et al.*, 2009; *Bloom et al.*, 2010] for which there is already a 7 year (2003–2009) time-series of global methane total column observations available with near-surface sensitivity [*Frankenberg et al.*, 2011; *Schneising et al.*, 2010].

[4] We report SWIR measurements of CH_4 from the Japanese Greenhouse Gases Observing SATellite (GOSAT) (section 2), the first dedicated greenhouse gas sensor, which can extend and improve the time-series obtained from SCIAMACHY. In section 3, we describe the optimal estimation retrieval process used to retrieve X_{CH4}. We compare these retrievals against correlative accurate/precise ground-based X_{CH4} data (section 4), and model data (section 5). We conclude the paper in section 6.

2. The Greenhouse Gases Observing SATellite (GOSAT)

[5] GOSAT was launched on 23 January 2009 [*Kuze et al.*, 2009] by the Japanese Space Agency and provides global measurements of total column CO_2 and CH_4 from its SWIR bands with global coverage every 3 days. It is equipped with two instruments: 1) the Thermal And Near Infrared Sensor for carbon Observations - Fourier Transform Spectrometer (TANSO-FTS) and 2) the Cloud and Aerosol Imager (TANSO-CAI).

[6] The TANSO-FTS instrument has four spectral bands with a high spectral resolution (0.3 cm^{-1}), three of which operate in the SWIR at around 0.76, 1.6 and 2.0 μm providing sensitivity to the near-surface absorbers with the fourth channel operating in the thermal infrared between 5.5 and 14.3 μm providing mid-tropospheric sensitivity.

[7] The measurement strategy of TANSO-FTS is optimized for the characterization of continental-scale sources and sinks. These measurements nominally consist of 5 across-track points, separated by ~100 km, with a ground footprint diameter of ~10.5 km and a 4 second exposure

[1]Earth Observation Science, Space Research Centre, University of Leicester, Leicester, UK.
[2]School of GeoSciences, University of Edinburgh, Edinburgh, UK.
[3]IUP, University of Bremen, Bremen, Germany.
[4]Centre for Atmospheric Chemistry, School of Chemistry, University of Wollongong, Wollongong, New South Wales, Australia.
[5]California Institute of Technology, Pasadena, California, USA.

Copyright 2011 by the American Geophysical Union.
0094-8276/11/2011GL047871

duration. Recent results from GOSAT include the preliminary validation of their CO_2 and CH_4 products against TCCON ground-based FTS instruments [*Morino et al.*, 2011].

3. GOSAT XCH_4 Retrieval Approach

[8] The OCO 'full physics' retrieval algorithm was developed for the NASA Orbiting Carbon Observatory (OCO) mission to retrieve X_{CO2} (dry-air column-averaged mole fraction of CO_2) from a simultaneous fit of SWIR O_2 and CO_2 bands. The OCO algorithm has been modified to operate on GOSAT spectra and we use it to perform global retrievals of X_{CH4}.

[9] The retrieval algorithm uses an iterative retrieval scheme based on Bayesian optimal estimation to retrieve a set of atmospheric/surface/instrument parameters, referred to as the state vector, from measured spectral radiances [*Boesch et al.*, 2011; *Connor et al.*, 2008]. The forward model, used to relate the state vector to the measured radiances, includes the LIDORT radiative transfer model combined with a fast 2-orders-of-scattering vector radiative transfer code [*Natraj et al.*, 2008]. In addition, we use the low-streams interpolation functionality of the code [*O'Dell*, 2010] to accelerate the radiative transfer component of the retrieval algorithm.

[10] For our GOSAT CH_4 retrieval, we have adopted the CO_2 proxy method [*Frankenberg et al.*, 2011]. CO_2 is known to vary in the atmosphere much less than CH_4 and as the CO_2 absorption band is spectrally close to that of CH_4 we can use the CO_2 as a proxy for the light path to minimize common spectral artefacts due to aerosol scattering and instrumental effects [*Butz et al.*, 2010]. CH_4 and CO_2 retrievals are carried out sequentially with channels at 1.65 μm and 1.61 μm respectively. In order to obtain a volume mixing ratio (VMR) of CH_4, it is necessary to multiply the X_{CH4}/X_{CO2} ratio by a model X_{CO2}. We obtain the CO_2 VMRs from the CarbonTracker model [*Peters et al.*, 2007], convolved with scene-dependent instrument averaging kernels obtained from the GOSAT CO_2 retrieval. The model data is normalized such that the annual global mean is consistent with our retrieved CO_2.

[11] The state vector of our retrieval consists of a 20-level profile for CH_4 and CO_2 VMRs, scaling factors for H_2O VMR and temperature profiles, surface albedo and a spectral shift/stretch. Details for the a priori can be found in the auxiliary material.[1] We process the latest versions of the GOSAT Level 1B files (050050C to 100100C) acquired via the GOSAT User Interface Gateway and apply the recommended radiometric calibration with the noise calculated from the standard deviation of the out-of-band signal. Spectra over ocean or with a signal-to-noise ratio below 50 are excluded.

[12] The spectroscopic parameters used for CO_2 and O_2 are taken from v3.2 of the OCO linelists which include line-mixing, whilst CH_4 and H_2O are taken from the TCCON linelists based on HITRAN08 [*Rothman et al.*, 2009] with updates to CO_2 [*Toth et al.*, 2008], H2O [*Toth*, 2005; *Jenouvrier et al.*, 2007] and CH_4 [*Frankenberg et al.*, 2008].

[13] Clouds shield parts of the atmosphere and consequently compromise the interpretation of retrieved X_{CH4}. To remove cloudy scenes, we first retrieve a clear-sky surface pressure from the O_2 A-Band which we compare to the ECMWF surface pressure interpolated to the measurement time and location. If they differ by more than 20 hPa we consider the scene to be cloudy and no X_{CH4} retrieval is performed.

[14] We examined a total of 1,101,442 GOSAT measurements performed over land between August 2009 and July 2010, which after filtering for signal-to-noise, cloud and data quality (currently χ^2 only) left 197,090 X_{CH4} retrievals (see auxiliary material for details).

4. Comparison to the Total Carbon Column Observing Network (TCCON)

[15] TCCON is a global network of ground-based high resolution Fourier Transform Spectrometers recording direct solar spectra in the near-infrared spectral region [*Wunch et al.*, 2011]. The overall objectives include improving the understanding of the carbon cycle and validating satellite retrievals by providing precise and accurate observations of X_{CO2} and X_{CH4} for a number of locations.

[16] Figure 1 shows all GOSAT retrievals along with the daily mean TCCON measurements of X_{CH4} for the period April 2009 to July 2010 over TCCON sites at Park Falls (USA, 45.95°N, 90.27°W), Lamont (USA, 36.60°N, 97.49°W), Darwin (Australia, 12.42°S, 130.89°E), Wollongong (Australia, 34.41°S, 150.88°E), Orleans (France, 47.97°N. 2.11°E) and Bialystok (Poland, 53.23°N, 23.03°E). These sites have been chosen with respect to their location, avoiding islands and hilly terrain and to obtain good latitudinal coverage (see map in Figure 3). The TCCON data uses GFIT Version 4.3.1 with GSETUP Version 2.7.4 and a CH_4 a priori profile with no geographical or temporal variation. TCCON columns are divided by a single, global factor of 0.978 ± 0.002 [*Wunch et al.*, 2011], based on calibration against aircraft overflights, to compensate for some systematic spectroscopic biases. No such factor is currently applied to the GOSAT retrievals, hence we may expect a systematic bias to TCCON measurements. In addition, the data for Wollongong and Darwin were produced using updated spectroscopic parameters which may lead to a 0.15% reduction in the X_{CH4}. Gaps in the TCCON data time-series are due to cloud and instrumental issues. In nominal mode, individual GOSAT measurements are spaced by ~100 km so that only a few GOSAT measurements are obtained directly in the proximity of a TCCON site. This situation is improved by GOSAT carrying out specific point observations over TCCON sites which increase the number of soundings over a small area. To compensate for the small number of GOSAT soundings directly over TCCON sites we include all cloud-free GOSAT measurements over land within ±5° of each TCCON site.

[17] To perform a quantitative comparison, if more than one GOSAT measurement over a TCCON site is available for a given day, we take the mean. Similarly, the mean of TCCON measurements within a 2 hour coincidence of these GOSAT measurements is taken, providing a single GOSAT and TCCON measurement per day. The difference and correlation coefficient given in Figure 1 are inferred from the above coincident daily-averaged measurements. The single-sounding precision is estimated from the standard deviation of the individual GOSAT-TCCON differences and we obtain values ranging from 7 to 15 ppb (0.4 to 0.8%) for the different sites.

[1] Auxiliary materials are available in the HTML. doi:10.1029/2011GL047871.

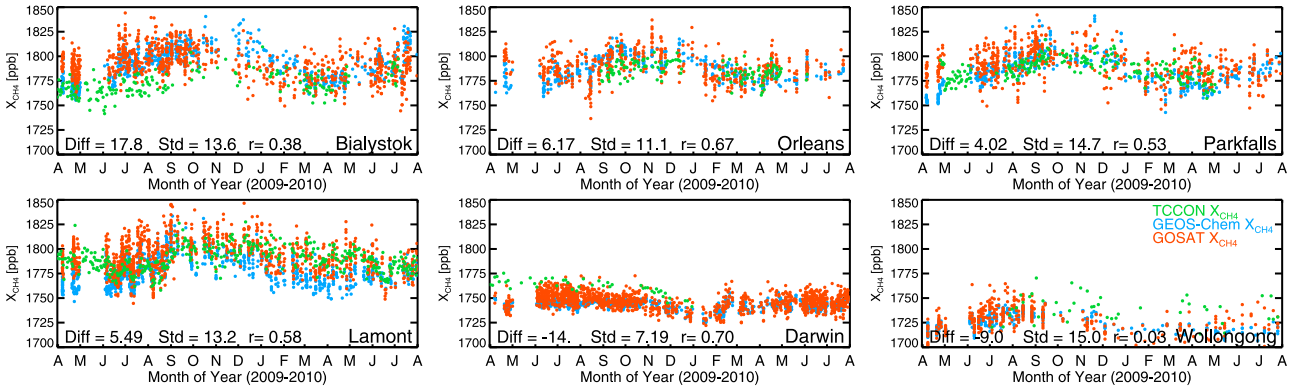

Figure 1. Time-series plots showing the GOSAT and GEOS-Chem X_{CH4} along with the daily mean TCCON X_{CH4} for the six TCCON sites; Bialystok, Orleans, Parkfalls, Lamont, Darwin and Wollongong. The GEOS-Chem data displayed has been convolved with the GOSAT scene-specific averaging kernels and thus is only intended for comparison to the GOSAT data. The difference (ppb) and correlation coefficient are inferred only for days where a 2 hour coincidence exists between TCCON and GOSAT observations. The single-sounding precision (ppb) is estimated by calculating the standard deviation of the individual GOSAT-TCCON differences.

[18] GOSAT observations generally reproduce the seasonal cycle observed by TCCON data at each site, with correlations calculated from daily data typically between 0.5 and 0.7. The two exceptions are Bialystok (r = 0.4) and Wollongong (where the correlation is insignificant). The amplitude of the seasonal cycle at Wollongong is small and the data are relatively sparse. Additionally, there are significant local methane sources (such as coal mining) as well as significant pollutant transport from Sydney such that a low correlation with GOSAT is not unexpected considering our spatial coincidence criteria. Additional scatter in the GOSAT retrieval could be due to local CO_2 sources which can impact the proxy retrieval.

[19] We find a latitudinal-dependent difference between the GOSAT X_{CH4} retrievals and the TCCON data which ranges from 17.9 ppb at the most northerly site (Bialystok) to −14.6 ppb at the site with the lowest latitude (Darwin).

[20] The ground based TCCON retrieval and the space-based GOSAT retrieval have been carried out using different a priori methane profiles and their vertical sensitivity as described by their averaging kernels will differ. Consequently the observed differences between the GOSAT and TCCON retrievals will include a contribution from smoothing error differences [*Rodgers and Connor*, 2003]. We assess the effect of the smoothing errors for GOSAT and TCCON retrievals by applying the averaging kernels for both retrievals to methane profiles from the GEOS-Chem model sampled for each sounding. The inferred mean smoothing error difference is largest for Bialystok and Orleans with values of 15.7 and 17.4 ppb respectively and smallest for Darwin with a value of 1.1 ppb. Taking into account this effect, we estimate that the biases in our GOSAT retrieval range from −17 to 2 ppb. A table with the results of the comparison is given in the auxiliary material.

5. Comparison to the GEOS-Chem Chemistry Transport Model

[21] We use the GEOS-Chem global 3-D chemistry transport model (v8-01-01), driven by GEOS-5 assimilated meteorology from the Global Modeling and Assimilation Office based at NASA Goddard, to relate CH_4 surface sources and sinks to atmospheric concentrations (A. Fraser et al., The Australian methane budget: Interpreting surface and train-borne measurements using a chemistry transport model, submitted to *Journal of Geophysical Research*, 2011). The 3-D meteorological data are updated every 6 hours and mixing depths and surface fields are updated every 3 hours. We use these data at a horizontal resolution of 2° latitude × 2.5° longitude, and with 47 hybrid vertical level ranging from the surface to the mesosphere, 30 of which are below 12 km.

[22] In the absence of more recent information, we use EDGAR and biomass burning from 2008 for 2009–2010; and use rice/wetland emissions from 2007 for 2008–2010 (see auxiliary material for details). Given the large uncertainties associated with any individual source estimates of CH_4 we anticipate that this assumption will only affect the magnitude and not the location of the emissions. The model is sampled at the time and location of individual GOSAT measurements, and is convolved with the GOSAT measurement specific averaging kernels.

[23] Figure 2 presents model and GOSAT monthly global distributions of X_{CH4} for September and December of 2009 and March and June of 2010; other monthly mean comparisons can be found in the auxiliary material. The resulting model and observed values range from 1680 ppb to 1810 ppb, with elevated values over known continental source regions of CH_4.

[24] There is very good ($0.93 \leq r \leq 0.99$) agreement between model and observed zonal mean hemispheric gradients, varying month to month, as expected with seasonal sources and sinks, with the model reproducing most of the observed variability.

[25] Differences between model and observed X_{CH4} values of up to 20 ppb are found over latitude bands which include strong emission sources. Figure 2 also shows model and GOSAT monthly spatial distributions. Large seasonal values over India and parts of southwest China, peaking in September, are due mainly to rice paddy emissions. We find large values over parts of Alaska, Canada and boreal Asia during northern hemisphere summer months, indicative of wetland

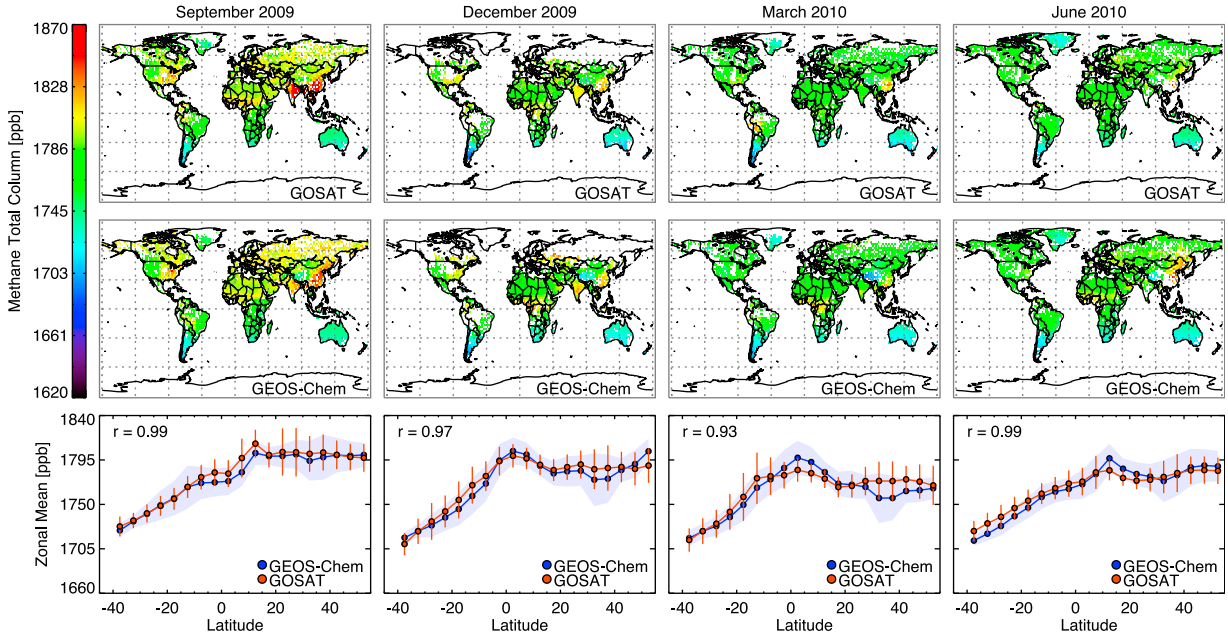

Figure 2. Monthly mean gridded 2° × 2° maps of the (top) GOSAT X_{CH4} and (middle) GEOS-Chem X_{CH4} for September 2009, December 2009, March 2010 and June 2010 sampled at the GOSAT measurement times and locations with the GOSAT scene-specific averaging kernel applied. (bottom) The zonal means between 40°S and 50°N in 5° bins for these months are also shown with the error bars (red) and shaded area (blue) represent the standard deviation of the GOSAT and GEOS-Chem data respectively. Also given is the correlation coefficient.

emissions and to a lesser extent wildfires. We also find elevated columns over known biomass burning regions (e.g., Africa, South America). As the relative enhancement in CH_4 and CO_2 due to biomass burning is similar, the proxy retrieval method may have reduced sensitivity to biomass burning emissions under certain conditions. Additionally, biomass burning emissions of CH_4 will be accompanied by combustion-related aerosol which may compromise the quality of retrieved columns and are removed by the cloud screening, helping to explain the relative sparseness of coverage over such regions.

[26] Figure 3 shows GOSAT and model X_{CH4} time-series, for the globe and for individual geographic regions of interest: southern Africa, northern Africa, Australia, the Amazon basin, North America, Southeast Asia, and Russia. The model and GOSAT global seasonal cycles, peaking in September and reaching a minimum in March with an amplitude of 25 ppb, agree to within a fraction of a percent with the model reproducing >92% of the observed variability.

[27] We have chosen contrasting geographical regions that reflect different seasonal sources. The model generally captures more than 70% of the observed variability, but can only capture half of the observed variability over the Amazon basin, which we attribute to known weaknesses in wetland emission models [e.g., *Bloom et al.*, 2010].

[28] The northern African region incorporates only minor sources and therefore provides our control, representing changes only in the seasonal CH_4 background due to the OH sink. For this region, we find a very high agreement ($r = 0.97$) in the magnitude and phase of X_{CH4} between the measurement and model. Australia, similarly, is relatively isolated from large-scale CH_4 sources and again we find consistency between model and measurement ($r = 0.85$) in capturing the small variability (amplitude of 20 ppb).

[29] North America, whilst including a range of sources, shows good agreement but with the amplitude of the seasonal cycle slightly higher (by ~10 ppb) in the model. The southern Africa region is dominated by wetland emissions and biomass burning. The model reproduces almost 70% of the variability observed by GOSAT but values tend to be smaller by ~10 ppb for most of the year.

[30] The strongest differences are observed for our Russia region, which extends from Finland, across Russia to eastern Siberia (incorporating boreal wetlands and biomass burning) and the Southeast Asia region, which includes emissions from rice cultivation over India and biomass burning. These CH_4 sources have a large seasonal pattern and we observe differences in the magnitude of these seasonal variations between model and observations of up to 20 ppb for the Russia region and up to 30 ppb for Southeast Asia, which reflects the high level of uncertainty of the emission inventories for this region. Despite these differences in the magnitude of the seasonal signals between measurement and model, the model is still able to capture 70% of the observed variability.

6. Concluding Remarks

[31] We present global CH_4 retrievals from GOSAT for August 2009 to July 2010 which we evaluate against correlative measurements from ground-based TCCON sites and calculations from the global 3-D GEOS-Chem chemistry transport model.

[32] From comparisons to TCCON observations we have inferred a single sounding precision for our CH_4 retrievals of 0.4 – 0.8% with estimated biases between −17 ppb and 2 ppb (0.1 to −0.9%) which is well within the mission targets of the GOSAT mission. We expect that the biases in the

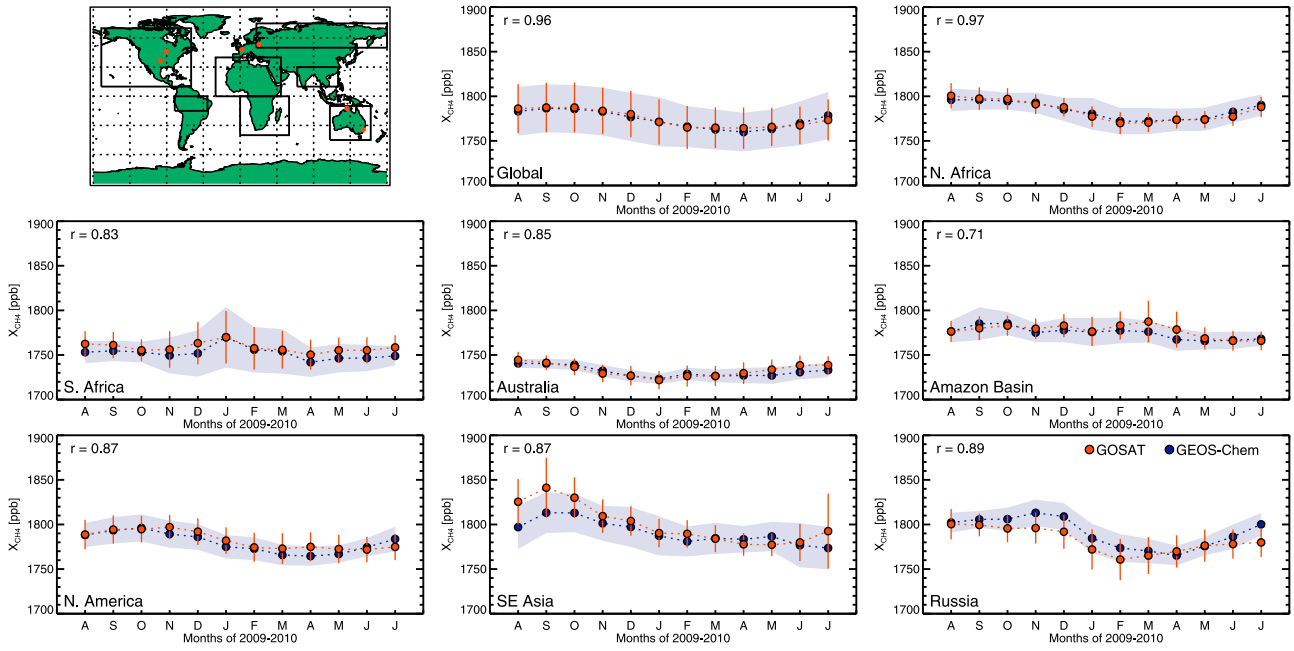

Figure 3. Time-series of the GOSAT and GEOS-Chem X_{CH4} between August 2009 and July 2010 globally and for the 7 regions outlined on the map. The error bars and shaded area represent the standard deviation of the GOSAT and GEOS-Chem data respectively. The location of TCCON sites used in section 4 are indicated by red dots.

retrieval can be reduced in the future by improvements in spectroscopy and instrument calibration. Potential biases in our retrieval might also be introduced by the use of a model CO_2 field as is required by the adopted proxy retrieval approach. Future work will have to focus on further improvements and continued validation of the X_{CH4} retrieval, but we expect that the performance of our current retrieval will be sufficient to provide information on the spatio-temporal distribution of CH_4 sources which can lead to improved estimates of CH_4 surface fluxes.

[33] We find a high level of consistency between our GOSAT X_{CH4} and large-scale features known to be well-represented by the model, such as the north-south gradient ($0.93 \leq r \leq 0.99$) and seasonal cycle over regions without significant sources (such as northern Africa where $r = 0.97$). While the model typically reproduces >70% of the variability observed with GOSAT, there are however clear differences in the magnitude of the seasonal patterns over known source regions (such as the Amazon ($r = 0.71$)) where the emission inventories are highly uncertain. These can be investigated further using an inverse model to quantify the corresponding flux estimates.

[34] **Acknowledgments.** We thank JAXA, NIES, and MOE for the GOSAT data and their continuous support as part of the Joint Research Agreement. R.P., L.F., and A.F. are supported by the NCEO and H.B. is supported by a RCUK fellowship. We also thank the OCO team at JPL for supplying the retrieval algorithm. We thank the BADC for providing ECMWF Operational Analyses data. TCCON is supported by NASA's Terrestrial Ecology Program through a grant to the California Institute of Technology. Operations support for Lamont and Darwin is provided by NASA's OCO. For the TCCON sites at Bialystok and Orleans, we thank AeroMeteo Service and the RAMCES team at LSCE for station maintenance and acknowledge the funding by the GOSAT team and within the EU-projects IMECC and GEOmon. We would also like to thank Geoff Toon for his advice and comments.

[35] The Editor thanks two anonymous reviewers for their assistance in evaluating this paper.

References

Bergamaschi, P., et al. (2009), Inverse modeling of global and regional CH_4 emissions using SCIAMACHY satellite retrievals, *J. Geophys. Res.*, *114*, D22301, doi:10.1029/2009JD012287.

Bloom, A. A., P. I. Palmer, A. Fraser, S. R. David, and C. Frankenberg (2010), Large-scale controls of methanogenesis inferred from methane and gravity spaceborne data, *Science*, *327*(5963), 322–325, doi:10.1126/science.1175176.

Boesch, H., D. Baker, B. Connor, D. Crisp, and C. Miller (2011), Global characterization of CO_2 column retrievals from shortwave-infrared satellite observations of the Orbiting Carbon Observatory-2 mission, *Remote Sens.*, *3*(2), 270–304, doi:10.3390/rs3020270.

Bousquet, P., et al. (2006), Contribution of anthropogenic and natural sources to atmospheric methane variability, *Nature*, *44*(7110), 439–443, doi:10.1038/nature05132.

Butz, A., O. P. Hasekamp, C. Frankenberg, J. Vidot, and I. Aben (2010), CH_4 retrievals from space-based solar backscatter measurements: Performance evaluation against simulated aerosol and cirrus loaded scenes, *J. Geophys. Res.*, *115*, D24302, doi:10.1029/2010JD014514.

Connor, B. J., H. Boesch, G. Toon, B. Sen, C. Miller, and D. Crisp (2008), Orbiting Carbon Observatory: Inverse method and prospective error analysis, *J. Geophys. Res.*, *113*, D05305, doi:10.1029/2006JD008336.

Dlugokencky, E. J., et al. (2009), Observational constraints on recent increases in the atmospheric CH_4 burden, *Geophys. Res. Lett.*, *36*, L18803, doi:10.1029/2009GL039780.

Frankenberg, C., T. Warneke, A. Butz, I. Aben, F. Hase, P. Spietz, and L. Brown (2008), Pressure broadening in the $2\nu3$ band of methane and its implication on atmospheric retrievals, *Atmos. Chem. Phys.*, *8*, 5061–5075, doi:10.5194/acp-8-5061-2008.

Frankenberg, C., I. Aben, P. Bergamaschi, E. Dlugokencky, R. Van Hees, S. Houweling, P. Van Der Meer, R. Snel, and P. Tol (2011), Global column-averaged methane mixing ratios from 2003 to 2009 as derived from SCIAMACHY: Trends and variability, *J. Geophys. Res.*, *116*, D04302, doi:10.1029/2010JD014849.

Jenouvrier, A., L. Daumont, L. Regalia-Jarlot, V. G. Tyuterev, M. Carleer, A. C. Vandaele, S. Mikhailenko, and S. Fally (2007), Fourier transform measurements of water vapor line parameters in the 4200-6600 cm-1 region, *J. Quant. Spectrosc. Radiat. Transfer*, *105*(2), 326–355, doi:10.1016/j.jqsrt.2006.11.007.

Kuze, A., H. Suto, M. Nakajima, and T. Hamazaki (2009), Thermal and near infrared sensor for carbon observation Fourier-transform spectrometer on the Greenhouse Gases Observing Satellite for greenhouse gases monitoring, *Appl. Opt.*, *48*(35), 6716–6733, doi:10.1364/AO.48.006716.

Morino, I., et al. (2011), Preliminary validation of column-averaged volume mixing ratios of carbon dioxide and methane retrieved from GOSAT

short-wavelength infrared spectra, *Atmos. Meas. Tech.*, *4*(6), 1061–1076, doi:10.5194/amt-4-1061-2011.

Natraj, V., H. Boesch, R. J. D. Spurr, and Y. L. Yung (2008), Retrieval of X_{CO2} from simulated Orbiting Carbon Observatory measurements using the fast linearized R-2OS radiative transfer model, *J. Geophys. Res.*, *113*, D11212, doi:10.1029/2007JD009017.

O'Dell, C. W. (2010), Acceleration of multiple-scattering, hyperspectral radiative transfer calculations via low-streams interpolation, *J. Geophys. Res.*, *115*, D10206, doi:10.1029/2009JD012803.

Peters, W., et al. (2007), An atmospheric perspective on North American carbon dioxide exchange: CarbonTracker, *Proc. Natl. Acad. Sci. U. S. A.*, *104*(48), 18,925–18,930, doi:10.1073/pnas.0708986104.

Rigby, M., et al. (2008), Renewed growth of atmospheric methane, *Geophys. Res. Lett.*, *35*, L22805, doi:10.1029/2008GL036037.

Rodgers, C. D. and B. J. Connor (2003), Intercomparison of remote sounding instruments, *J. Geophys. Res.*, *108*(D3), 4116, doi:10.1029/2002JD002299.

Rothman, L. S., et al. (2009), The HITRAN 2008 molecular spectroscopic database, *J. Quant. Spectrosc. Radiat. Transfer*, *110*(9–10), 533–572, doi:10.1016/j.jqsrt.2009.02.013.

Schneising, O., M. Buchwitz, M. Reuter, J. Heymann, H. Bovensmann, and J. P. Burrows (2010), Long-term analysis of carbon dioxide and methane column-averaged mole fractions retrieved from SCIAMACHY, *Atmos. Chem. Phys. Discuss.*, *10*(11), 27,479–27,522, doi:10.5194/acpd-10-27479-2010.

Toth, R. (2005), Measurements of positions, strengths and self-broadened widths of H_2O from 2900 to 8000 cm^{-1}: Line strength analysis of the 2nd triad bands, *J. Quant. Spectrosc. Radiat. Transfer*, *94*(1), 51–107, doi:10.1016/j.jqsrt.2004.08.042.

Toth, R., L. Brown, C. Miller, V. Malathy Devi, and D. Benner (2008), Spectroscopic database of CO_2 line parameters: 4300–7000cm- 1, *J. Quant. Spectrosc. Radiat. Transfer*, *109*(6), 906–921, doi:10.1016/j.jqsrt.2007.12.004.

Wunch, D., G. C. Toon, J.-F. L. Blavier, R. A. Washenfelder, J. Notholt, B. J. Connor, D. W. T. Griffith, V. Sherlock, and P. O. Wennberg. (2011), The total carbon column observing network, *Philos. Trans. R. Soc. A*, *369*, 2087–2112, doi:10.1098/rsta.2010.0240.

H. Boesch, A. Cogan, and R. Parker, Earth Observation Science, Space Research Centre, University of Leicester, University Road, Leicester LE1 7RH, UK.

N. Deutscher, J. Messerschmidt, and J. Notholt, IUP, University of Bremen, Bremen D-28334, Germany.

L. Feng, A. Fraser, and P. I. Palmer, School of GeoSciences, University of Edinburgh, Edinburgh EH9 3JN, UK.

D. W. T. Griffith, Centre for Atmospheric Chemistry, School of Chemistry, University of Wollongong, Wollongong, NSW 2522, Australia.

P. O. Wennberg and D. Wunch, California Institute of Technology, Pasadena, CA 91125, USA.